IEEE Access
Multidisciplinary ⋮ Rapid Review ⋮ Open Access Journal

Received March 27, 2021, accepted April 28, 2021, date of publication May 7, 2021, date of current version May 19, 2021.
Digital Object Identifier 10.1109/ACCESS.2021.3078150

Neutrosophic Rayleigh Model With Some Basic Characteristics and Engineering Applications

ZAHID KHAN[1], MUHAMMAD GULISTAN[1], NASREEN KAUSAR[2], AND CHOONKIL PARK[3]
[1]Department of Mathematics and Statistics, Hazara University Mansehra, Mansehra 21120, Pakistan
[2]Department of Mathematics, University of Agriculture, Faisalabad 38000, Pakistan
[3]Department of Mathematics, Research Institute for Natural Sciences, Hanyang University, Seoul 04763, South Korea

Corresponding authors: Choonkil Park (baak@hanyang.ac.kr) and Zahid Khan (zahidkhan@hu.edu.pk)

This work was supported by the Basic Science Research Program through the National Research Foundation of Korea by the Ministry of Education, Science and Technology under Grant NRF-2017R1D1A1B04032937.

ABSTRACT The fundamentals of neutrosophic statistics provide a new basis for working with indeterminate data problems. In this study, the notion of the neutrosophic Rayleigh distribution (RD_N) has been introduced. The neutrosphic extension of the classical Rayleigh model with several application areas is highlighted. The major characteristics of the proposed distribution are described in a way that suggested model can be utilized in different situations involving undetermined, vague and fuzzy data. The usage of proposed distribution notably in the domain of statistical process control (SPC) is considered. The classical structure of V_{SQR}-chart is not capable of capturing uncertainty on studied variables. The mathematical structure of the V_{NR}-chart based on the proposed neutrosophic distribution has been developed. The neutrosphic parameters of the proposed V_{NR}-chart with other related performance metrics such as neutrosophy run length (ARL_N) and neutrosophy power curve (PC_N) are established. The proposed chart's performance in a neutrosophic environment is also evaluated to the existing model. Results from this comparative analysis reveal that the suggested $\mathrm{V_{NR}}$-chart outperforms its current equivalent in terms of neutrosophic statistical power. Finally, a charting structure of proposed design for service life of ball bearings data is considered with a view to support implementation procedure of the proposed neutrosophic design in real-world scenarios.

INDEX TERMS Neutrosophic logic, Rayleigh model, control chart, neutrosophic parameters.

I. INTRODUCTION

Variability is an inevitable phenomenon of the production industry. It is often due to normal causes and specific causes of variation. Quality management utilizes different management and engineering methods to manufacture quality goods by eliminating abnormal rooted variations [1]. The process operating only under irregular variations is considered out-of-control (OC) and the process working underlying normal causes of variation is called in-control (IC) in statistical terms. The SPC is a common technique that involves statistical tools to precisely measure variations in the parameters of the production or manufacturing process [2]. A statistical quality control chart, an effective technique in the SPC, is commonly practiced in service and manufacturing industries to analyze the behavior of processes in addition to enhancing their productivity [3]. The primary aim of the control chart is to identify irregularity in manufactured items as soon as possible, so that the process could be terminated on time before the manufacturing of faulty products [4]. The Shewhart chart, originally introduced by Walter A. Shewhart, is a very trendy process predictive method that can be implemented and interpreted easily. Due to its easy implementation and broad usage, the Shewhart chart is not frequently used in service industries and modern processes where minor process changes can impose severe financial losses [5]. It is therefore vital to use memory-type charts that are more responsive to moderate-to-small changes in the target parameters [6]. On the contrary, SPC problems may involve uncertainty, as are most of the true world systems. When there is uncertainty in the system and even if the quality characteristics are portrayed by human perception, the process cannot be precisely described by control charts mentioned above [7]. In order to explain and model such problems, fuzzy set theory is therefore used [8]. A brief application of fuzzy charts can be originated in studies [9]–[11]. The fuzzification based control charts are more sensitive in general than standard control charts [8]. The idea of Neutrosophic Set (NS) is a broader

The associate editor coordinating the review of this manuscript and approving it for publication was Aniruddha Datta.

platform that expands the notions of the fuzzy and classical sets [12].

The occurrence of truth, false and indeterminate situations are considered in the philosophy of the NS. The notion of the NS is now extended to various fields of study [13]. There are several real-world circumstances where the collected data might be indeterminate. For applications containing imprecise data are handled by different researchers using the neutrosophic statistics (NST) [14]–[16]. The classical approach of the conventional statistical techniques has been generalized in the area of NST with the purpose to deal with vagueness in processing data. It is not possible to use a traditional control chart approach when underlying data consists of Incomplete, vague, or uncertain data on quality characteristics. Statistical methods integrated with the neutrosophic logic have been recently developed in the literature of SPC by numerous researchers such as Aslam proposed the neutrosphic version of the acceptance sampling plan in the domain of SPC [17]. Aslam and Raza suggested a sampling plan for several production lines employing the NST [18]. Whereas the more facts on the usage of NST in structuring the Shewhart charts can be found in [18]–[22]. When normality presumption is severely violated, the application of widely used control charts is drastically less prudent. The V_{SQR} is one of such designs to accommodate this non-normality situation for quality data that best described by the classical Rayleigh model [23]. Rayleigh distribution (RD) is one of the statistical distributions that attracted various researchers due to its applications in vast engineering related problems [24], [25].

In this work, we are intended to describe some characteristics of the RD_N and the neutrosophic extension of the V_{SQR}-chart that can deal the indeterminate observations in Rayleigh distributed quality characteristics. The proposed V_{NR} design is rooted on the RD_N and represents the generalization of the conventional V_{SQR}-chart.

The remainder of the study is arranged as follows: Section 2 provides the introduction of the RD_N. The suggested control chart based on the RD_N is given in Section 3. The performance measure of the proposed neutrosophic design is described in Section 4. A comparison study of the V_{NR} design is given in Section 5. A real example of the functional implementation of the proposed V_{NR}-chart has been explained in Section 6. The main results of the research are outlined and concluded in Section 7.

II. NEUTROSOPHIC RAYLEIGH MODEL

Definition: The Neutrosophic model of the Rayleigh distribution with imprecision in the scale parameter θ_N has the following characteristics:

$$\mathrm{f}(z, \theta_N) = \frac{Z}{\theta_N^2} e^{-\frac{1}{2}\left(\frac{Z}{\theta_N}\right)^2}, \theta_N > 0, Z > 0. \tag{1}$$

$$F(Z, \theta_N) = 1 - e^{-\frac{1}{2}\left(\frac{Z}{\theta_N}\right)^2}, \theta_N > 0, Z > 0. \tag{2}$$

where $\theta_N \in [\theta_l, \theta_u]$, $\mathrm{f}(z, \theta_N)$ and $F(z, \theta_N)$ denote the neutrosophic density function ($\mathrm{PDF_N}$) and characteristic function (CDF_N) respectively of the RD_N. Based on the neutrosophic version of the Rayleigh model primary characteristics of the neutrosophic random Z are given by:

$$\mu_N = \theta_N \sqrt{\frac{\pi}{2}}, \sigma_N^2 = \theta_N^2 \left(2 - {}^{\pi}/_{2}\right)^2 \tag{3}$$

where μ_N and σ_N^2 are mean and variance respectively of the RD_N.

The graphical expressions of the $f(z, \theta_N)$ and $F(z, \theta_N)$ for the neutrosphic Rayleigh variable Z with imprecise parameter $\theta_N = [0.5, 0.75]$ is shown in the Figure 1.

From the plot in Figure 1(a) the neutrosophic region can be seen with shaded region between the dotted lines and curve is asymmetric curve for the indeterminate value [0.5, 0.75] of the scale parameter θ_N. An infinite number of structures is possible for the PDF_N, since the neutrosophic scale parameter affects the form of the curve. However the large value of θ_N may result in the symmetric behavior of the $\mathrm{PDF_N}$. Figure 1 (b) denotes the typical non-decreasing behavior of the underlying CDF_N curve for the same selected values of the θ_N which is one of the most general descriptions of a distribution function.

Rayleigh distribution is widely employed to describe the wind speed data, signals data in communications, lifetimes of different objects in reliability studies, modeling the noise factor in magnetic imaging and in SPC for designing the control chart structure that may employ for monitoring the stability of the distribution parameter. Here are a few examples of neutrosophic version of the Rayleigh distribution for the purpose to underline its significant in a variety of fields.

Example 1: Let the neutrosophic Rayleigh distribution as defined in (1) is used to describe the repair time in hours of a manufacturing machine with mean time [30, 45] hours. Determine the probability that repair time does not exceed 35 hours.

Solution: Given that $\mu_N = [30, 45]$ so by using relation given in (3) we can get neutrosophic scale parameter $\theta_N \cong [24, 36]$.

Now using (2), we have found the desired probability as:

$$\begin{aligned} P(Z \leq 35) &= 1 - e^{-\frac{1}{2}\left(\frac{z}{\theta_N}\right)^2} \\ &= 1 - e^{-\frac{1}{2}\left(\left[\frac{35}{36}, \frac{35}{24}\right]\right)^2} \\ &= 1 - e^{-[0.472, 1.063]} \end{aligned}$$

Example 2: Let the daily electricity consumption in different estates of KPK province in Pakistan is a neutrosphic random variable Z which is best described by $\mathrm{PDF_n}$ as given in (1) with neutrosophic scale parameter $\theta_N = [1000, 1500]$.

The power plants of this province have a capacity of 2762 Megawatt (MW). On any given day, what is the probability that power supply would be inadequate?

Solution: Power supply will be inadequate if demand of power is more than installed capacity

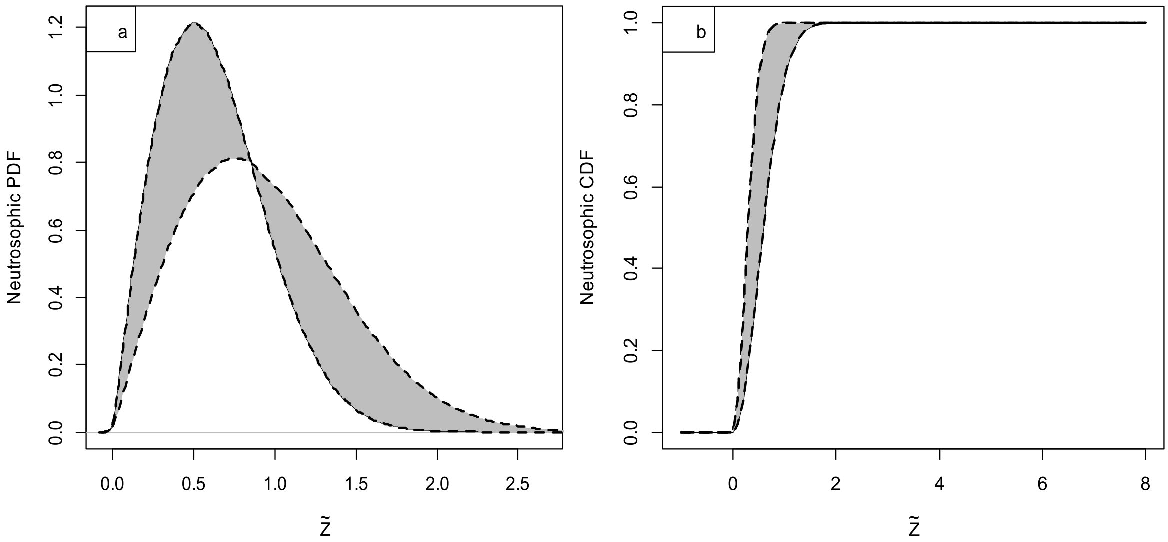

FIGURE 1. ***PDF$_N$* and *CDF$_N$* of the neutrosophic Rayleigh random variable.**

It follows:

$$\begin{aligned} P(Z>2762) &= 1-P(Z\leq 2762)\\ &= 1-e^{-\frac{1}{2}\left(\frac{2762}{[1000,1500]}\right)^2}\\ &= [0.816, 0.978] \end{aligned}$$

Hence the approximate probability of insufficient supply will be within 0.82 to 0.98.

III. PROPOSED CONTROL CHART

In this section proposed chart based on the RD_N has been proposed. The value of the characterized neutrosophic scale parameter θ_N is typically not determined in real-life scenarios. Several estimation techniques may be used to find the unknown quantity σ [26]. Based on the maximum likelihood (ML) strategy, an estimate of θ_N is provided by [23]:

$$\hat{\theta}_N = \sqrt{\frac{\sum_{i=1}^{\tilde{m}} X_{iN}^2}{2\tilde{m}}}. \tag{4}$$

where $\tilde{m} = [m_L, m_U]$ is the neutrosophic sample size which turn to classical sample size when $m_L = m_U = m$.

We need to identify the distribution of the neutrosophic $\hat{\theta}_N$-statistic for structuring the parameters of the proposed V_N-chart. The statistic $\hat{\theta}$ is connected with the chi (χ) random variable V as follows [23]:

$$\hat{\theta}_N = \frac{\sigma}{\sqrt{2m}}V \tag{5}$$

where V follows χ-distribution with $2m$ degree of freedom (df). Now it has been assumed that imprecise values of σ and m are given rather than crisp values.

Equation (5) can be rewritten under the neutrosophic condition as:

$$\hat{\theta}_N = \frac{\sigma_N}{\sqrt{2\tilde{m}}}\tilde{V} \tag{6}$$

where random variable $\tilde{V}$ follows the neutrosophic χ-distribution (χ_N) with $2\tilde{m}df$.

Utilizing (6) the neutrosophic characteristics of the estimator $\hat{\theta}_N$ can be found as:

$$\left.\begin{aligned} E\left(\hat{\theta}_N\right) &= \sigma_N A(\tilde{m})\\ V\left(\hat{\theta}_N\right) &= \sigma_N^2\left[1-A(\tilde{m})^2\right] \end{aligned}\right\} \tag{7}$$

where $A(\tilde{m}) = \frac{1}{\sqrt{(\tilde{m})}}\frac{\Gamma\left((\tilde{m})+\frac{1}{2}\right)}{\Gamma(\tilde{m})}$ is constant and based on the neutrosophic sample size $\tilde{m}$.

Equation (7) indicates that statistic $\hat{\theta}_N$ is biased estimator of σ_N. Suppose that k sample batches with imprecise values are provided for analysis and $\hat{\theta}_{Ni}$ be the ML statistic of the ith sample batch then average defined on all k sample batches would be:

$$\bar{\theta}_N = \frac{\sum_{i=1}^{k}\hat{\theta}_{Ni}}{k} \tag{8}$$

Following (7) and (8) the σ_N can be estimated by an unbiased estimator as:

$$\hat{\sigma}_N = \frac{\bar{\theta}_N}{A(\tilde{m})} \tag{9}$$

The distribution of $\hat{\theta}_N$ is asymmetric specifically for smaller values of $\tilde{m}$, so 3-sigma limits are not generally applicable due to unequal tail areas [27]. Probability limits (PL) are readily used to deal with this issue as a standard practice in SPC.

As $\tilde{V}$ follows the neutrosophic chi distribution with $2\tilde{m}df$, αth percentage point of the distribution is defined as:

$$F_\chi(\tilde{v}) = \alpha \tag{10}$$

Consequently simplification of (10) and (5) follows

$$\hat{\theta}_N = \frac{\sigma_N}{\sqrt{2\tilde{m}}}F_\chi^{-1}(\alpha) \tag{11}$$

Thus the PL of the proposed V_N-chart are then obtained by:

$$\left.\begin{aligned} \tilde{UPL} &= \frac{\sigma_N}{\sqrt{2\tilde{m}}} F_\chi^{-1}\left(1-\frac{\alpha}{2}\right) = \sigma_N \tilde{Q}_1 \\ \tilde{LPL} &= \frac{\sigma_N}{\sqrt{2\tilde{m}}} F_\chi^{-1}\left(\frac{\alpha}{2}\right) = \sigma_N \tilde{Q}_2 \end{aligned}\right\} \quad (12)$$

where $\tilde{Q}_1 = \frac{F_\chi^{-1}(1-\frac{\alpha}{2})}{\sqrt{2\tilde{m}}} = [Q_{1L}, Q_{1U}]$ and $\tilde{Q}_2 = \frac{F_\chi^{-1}(\frac{\alpha}{2})}{\sqrt{2\tilde{m}}} = [Q_{2L}, Q_{2U}]$.

When the parameter of the distributed quality characteristic of the RD_N is not specified, it would be calculated using an estimator given in (9). Thus PL based on the estimated parameters can be modified as:

$$\left.\begin{aligned} \tilde{UPL} &= \frac{\hat{\sigma}_N}{\sqrt{2\tilde{m}}} F_\chi^{-1}\left(1-\frac{\alpha}{2}\right) = \bar{\theta}_N \tilde{Q}_3 \\ \tilde{LPL} &= \frac{\hat{\sigma}_N}{\sqrt{2\tilde{m}}} F_\chi^{-1}\left(\frac{\alpha}{2}\right) = \bar{\theta}_N \tilde{Q}_4 \end{aligned}\right\} \quad (13)$$

where $\tilde{Q}_3 = \frac{F_\chi^{-1}(1-\frac{\alpha}{2})}{A(\tilde{m})\sqrt{2\tilde{m}}} = [Q_{3L}, Q_{3U}]$ and $\tilde{Q}_4 = \frac{F_\chi^{-1}(\frac{\alpha}{2})}{A(\tilde{m})\sqrt{2\tilde{m}}} = [Q_{4L}, Q_{4U}]$

The classical pair of crisp values (Q_1, Q_2) and (Q_3, Q_4) for fixed risk factor α and at various values of $\tilde{m}$ are easily calculated and available in [23]. The 3-sigma limits can be developed in a similar fashion, however are not focused here because of asymmetric behavior of the underlying statistic $\hat{\theta}_N$ particular for a smaller indeterminate values of $\tilde{m}$.

IV. PERFORMANCE ANALYSIS

In this section, the performance metrics used in this study have been described, followed by a comparative analysis, and outlined their computational algorithm. To evaluate the sensitivity of the proposed V_{NR}-chart the notions of the neutrosophic operating characteristic curve (OC_N), ARL_N and PC_N are described. There are widely used metrics to assess the efficiency of proposed design in classical control charts theory [28]. The OC_N and PC_N functions are customary employed to characterize the control chart's ability to detect a difference in the observed quality phase. The ARL_N statistic, on the other hand, describes the average samples taken prior to the identification of abrupt change in the target parameter for a system operating under any special cause. The control chart method is similar to the hypothesis evaluation strategy, so, the V_NR-chart's ability to not detect change in target parameter would be defined in accordance with neutrosophic type II error as follows:

$$\beta_N = P\left[\tilde{LCL} \le \hat{\theta}_N \le \tilde{UCL}\,|H_1\right] \quad (14)$$

Here H_1:$\sigma_\text{N} = \sigma_{\text{N}1}$ stands for alternative hypothesis with $\sigma_{\text{N}1} = \delta\sigma_{\text{N}0}$, δ is shift constant and $\sigma_{\text{N}0} = [\sigma_{\text{L}0}, \sigma_{\text{U}0}]$ is neutrosophic IC target parameter of the RD_N.

Equation (14) further can be written as:

$$\beta = F_\chi\left(\delta\tilde{Q}_1\sqrt{2\tilde{m}}\right) - F_\chi\left(\delta\tilde{Q}_2\sqrt{2\tilde{m}}\right) \quad (15)$$

where F_χ is distribution function of the χ_N with $2\tilde{m}$df.

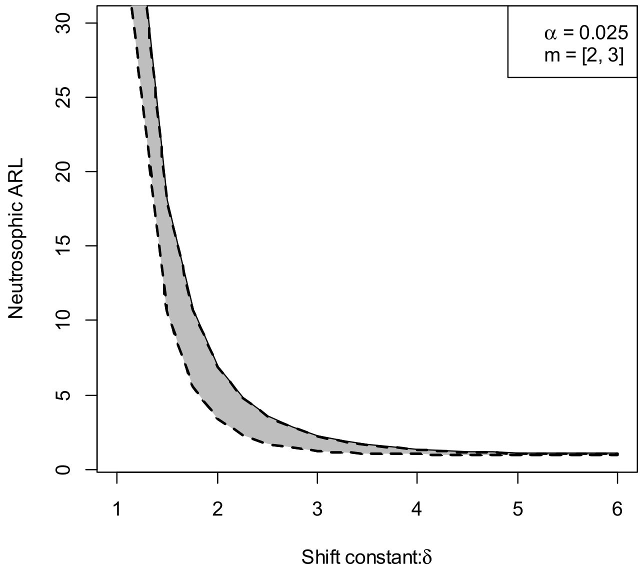

FIGURE 2. **Construction of the $\text{ARL}_{\text{N}1}$ for V_{NR}-chart.**

Using (15) $\text{ARL}_{\text{N}1}$ for OC process can be expressed as:

$$ARL_1 = \frac{1}{1 - F_\chi\left(\delta\tilde{Q}_1\sqrt{2\tilde{m}}\right) + F_\chi\left(\delta\tilde{Q}_2\sqrt{2\tilde{m}}\right)} \quad (16)$$

where $1 - F_\chi\left(\delta\tilde{Q}_1\sqrt{2\tilde{m}}\right) + F_\chi\left(\delta\tilde{Q}_2\sqrt{2\tilde{m}}\right) = 1 - \beta$ constitutes the power of the proposed V_{NR}-chart.

Note that the shift constant values $\delta > 1$ and $\delta < 1$ in (16) determine the downward and upward shifts respectively in the monitoring parameter whereas the value $\delta = 1$ stands for a process working at the target value σ_{N0}. In order to determine the use of (16), let's assume $\delta > 1$ and we are trying to work out how many samples are expected on average to identify a specific shift.

The ARL_N curve is provided in Figure 2 for the proposed chart for a neutrosophic sample size $\tilde{m} = [2, 3]$ at $\alpha = 0.025$.

Figure 2 represents the geometric shape of the run length distribution for a particular neutrosophic sample size $\tilde{m}$ and variety of curves can be constructed in similar way for other values of $\tilde{m}$. The curve in Figure 2 would be helpful to determine the average number samples needed for a particular shift in the target parameter. As an example, consider a shift of quantity $2\sigma_{N0}$ in the target parameter, on average [4, 6] samples would be required to initiate this particular shift. Besides that, if we increase the shift size, this ARL_{N1} tends to constant value 1. For a better clarity, the proposed design's run length characteristic is also evaluated at different sample sizes in Table 1 with fixed false alarm rate $\alpha = 0.025$.

Results in Table 1 indicate that the measured ARL_{N1} value is closer to the expected value of 40, particularly when the sample size is greater and the process is IC i.e., $\delta = 1$. The V_{NR}-chart is extremely effective for determining moderate to large changes in the target parameter, as observed by these ARL_{N1} values. Additionally, by changing the neutrosophic target parameter to σ_{N1}, the performance of the V_{NR}-chart in terms of PC_N function can be evaluated for different values

TABLE 1. The ARL_N profile of the proposed chart.

Shift constant (δ)	Neutrosophic Sample Size ($\tilde{m}$)		
	[2, 3]	[4, 6]	[7, 9]
	ARL_N		
1.00	[39.81,39.99]	[39.95, 40.15]	[40.04, 40.08]
1.50	[10.69, 18.11]	[4.00, 7.18]	[2.30, 3.21]
2.00	[3.37, 6.90]	[1.32, 2.13]	[1.05, 1.17]
2.50	[1.75, 3.56]	[1.02, 1.25]	[1.00, 1.00]
3.00	[1.25, 2.25]	[1.00, 1.05]	[1.00, 1.00]
3.50	[1.08, 1.65]	[1.00, 1.00]	[1.00, 1.00]
4.00	[1.02, 1.33]	[1.00, 1.00]	[1.00, 1.00]
4.50	[1.00, 1.17]	[1.00, 1.00]	[1.00, 1.00]
5.00	[1.00, 1.09]	[1.00,1.00]	[1.00, 1.00]

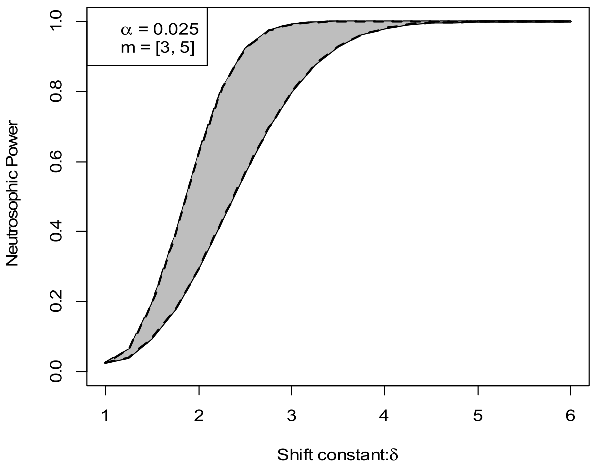

FIGURE 3. The neutrosophic power curve.

of $\tilde{m}$ and α. For example, the PC_N computed for $\tilde{m} = [3, 5]$ with false rate $\alpha = 0.025$ is shown in Figure 3.

The neutrosophic power plot in Figure 3 also reveals that the proposed V_{NR} control chart essentially detects various amounts of changes in the monitoring parameter. This curve, provides the power platform of the proposed chart for detecting a certain amount of shift in the monitoring parameter. For instance, the V_{NR}-chart provides neutrosophic power in range of [0.799, 0.993], for detecting a shift of $3\sigma_{N0}$ in scale parameter of the RD_N.

V. COMPARISON ANALYSIS

In this part, the proposed chart's performance is compared to other existing design used for monitoring the neutrosophic parameter of the RD_N. The performance of V_{NR}-chart has been compared with existing model of the V_{SQR}-chart under the indeterminate environment.

For this comparison, a number of available metrics can be used; however, power curves are commonly used in several studies [29], [30]. The proposed chart power in (16) is the probability of accurately rejecting H_0. In our case, the power of the V_{NR}-chart is characterized if the calculated statistics ($\hat{\theta}_{Ni}$) exceed the lower and upper calculated limits for a given value of false alarm probability α and neutrosophic sample size $\tilde{m}$. Any control chart that has a higher probability of appropriately rejecting H_0 is deemed efficient. The power of the suggested chart and its equivalent V_{SQR} has been estimated using this method for fixed values of α and $\tilde{m}$ in Figure 4.

Neutrosophic power curves in Figure 4 show that power of both charts increase with increased in shift constant i.e., $\delta > 1$. When the process is under control with a shift constant = 1, the power is even similar to the theoretical false rate probability $\alpha = 0.025$. For each shift in scale parameter power is given in an imprecise range and represented by the shaded region. For instance, power of the V_{NR} control is about [0.4, 0.85] for detecting a shift of amount 3 at $\tilde{m} = [2, 4]$ whereas existing design has approximately neutrosophic power in range [0.30, 0.65] for the same shift in the target parameter. If the sample size becomes larger, the disparity becomes larger. Thus, it is obvious from Figure 4 that the proposed V_{NR}-chart is more capable than the neutrosophic V-chart for detecting shifts in the parameter σ_{N0} for a given value of $\tilde{m}$.

TABLE 2. Neutrosophic ball bearings failure life data.

S. No	x_{N1}	x_{N2}	x_{N3}	$\hat{\theta}_N$
1	[0.70, 0.81]	[0.67, 0.73]	[0.80, 0.86]	[0.51, 0.57]
2	[0.63, 0.81]	[0.96, 1.04]	[1.06, 1.21]	[0.63, 0.73]
3	[0.35, 0.41]	[1.07, 1.26]	[0.60, 0.70]	[0.52, 0.61]
4	[0.70, 0.72]	[0.95, 1.35]	[0.85, 1.01]	[0.59, 0.75]
5	[1.12, 1.43]	[0.82, 1.02]	[0.34, 1.11]	[0.58, 0.85]
6	[0.47, 1.39]	[0.23, 0.74]	[0.07, 1.17]	[0.52, 0.80]
7	[0.85, 1.03]	[0.76, 0.95]	[0.41, 0.44]	[0.49, 0.60]

VI. REAL APPLICATION

In this part, a real data set has been utilized to demonstrate the computational procedure of the suggested chart illustrated in Section 3. Data used in analysis is originally analyzed by Lieblein and Zelen [31] with a view to model the service life of ball bearing data. Data is further analysis by many other others in their respective studies [32], [33]. The observations in this dataset represent the revolution (in million) of 23 ball bearing balls before failure occurred. The ball bearing data fits well with the Rayleigh distribution as discussed in [34]. Here this dataset collection is examined from the viewpoint of a neutrosophic environment. The data from the original source are exact numerical values, but neutrosophic data are produced according to the method reported in [20] to aid in understanding the preceding concept of the V_N-chart. The data produced in this way is now available in ranges rather than crips values. The indeterminate data in ranges on ball bearing failure times are divided into seven subgroups, each with three observations listed in Table 2. The neutrosophic statistic $\hat{\theta}_N$ is used in the proposed control chart to monitor the target parameter of the RD_N. As a result, the statistic $\hat{\theta}_N$ for each subgroup is calculated and recorded in the fourth column of Table 2.

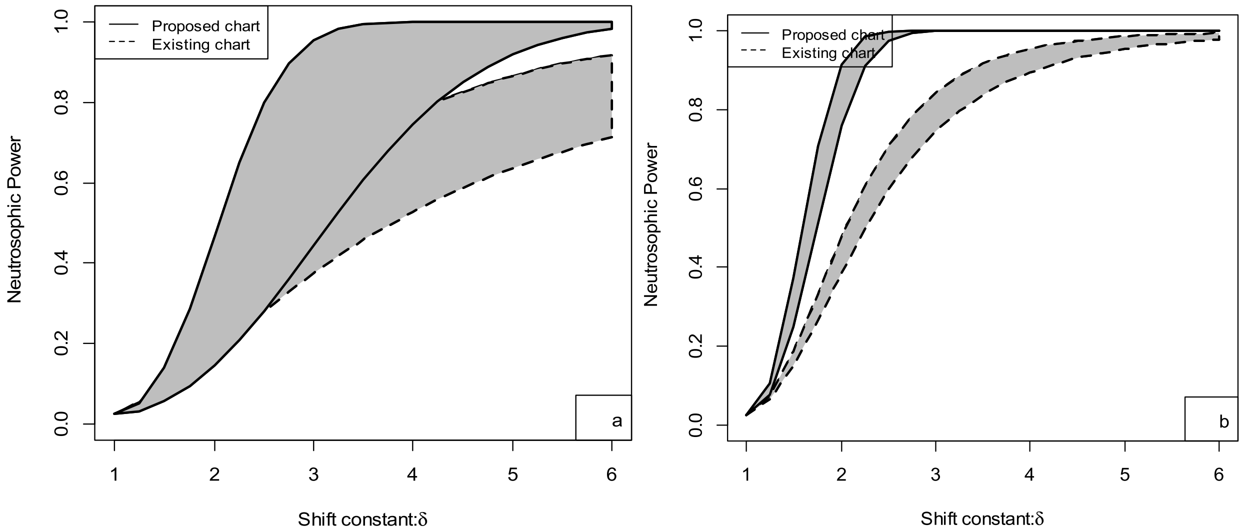

FIGURE 4. Power comparisons at $\alpha = 0.025$ and (a) neutrosophic sample size $\tilde{m} = [2, 4]$ and (b) neutrosophic sample size $\tilde{m} = [6, 8]$.

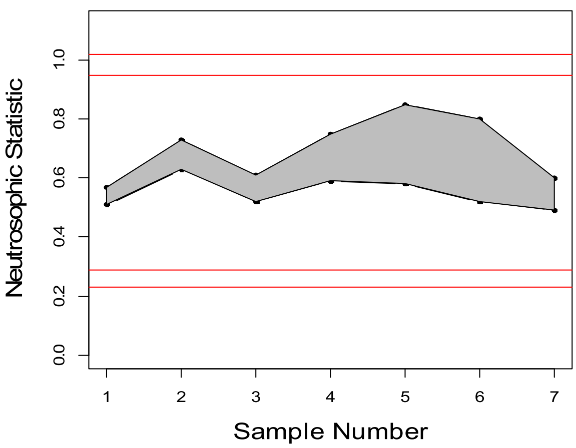

FIGURE 5. The construction of V_{NR} control chart for ball bearings life times data.

For the details in Table 3, the parameters of the V_{NR} control chart utilizing (13) are obtained as follows:

$$\tilde{UPL} = [0.95, 1.02], \quad CL = [0.55, 0.70] \quad \text{and } \tilde{LPL} = [0.23, 0.29].$$

Figure 5 shows a schematic representation of the proposed V_N control for the observed quality characteristic.

The plotted neutrosophic statistics in Figure 5 have a random behavior and are within the control limits. Consequently, observed process may be inferred as in a state of statistical control.

VII. CONCLUSION

In this work, the classical Rayleigh model has been extended in accordance with neutrosophic logic. Mathematical characteristics of the proposed distribution under an indeterminacy environment are described. Application areas of the RD_N have been provided for working data that contain vague, indeterminate and imprecise observations on studied variables. A new control chart based on the proposed RD_N is developed due to its adequacy of dealing vague data in the applications of SPC. The neutrosophic parameters, ARL_N, PC_N and OC_N of the suggested chart have been derived. To illustrate the theoretical results, a simulation study is carried out and performance of the V_N-chart is compared with existing counterpart. Numerical results illustrate that proposed design is more effective in terms of identifying changes in the monitoring parameter of the RD_N.

REFERENCES

[1] Z. Abbas, H. Z. Nazir, N. Akhtar, M. Riaz, and M. Abid, "An enhanced approach for the progressive mean control charts," *Qual. Rel. Eng. Int.*, vol. 35, no. 4, pp. 1046–1060, Jun. 2019.

[2] K. F. Sellers, "A generalized statistical control chart for over-or under-dispersed data," *Qual. Rel. Eng. Int.*, vol. 28, no. 1, pp. 59–65, Feb. 2012.

[3] A. Haq, M. Bibi, and B. A. Shah, "A novel approach to monitor simple linear profiles using individual observations," *Commun. Statist.-Simul. Comput.*, pp. 1–14, Jul. 2020, doi: 10.1080/03610918.2020.1799229.

[4] M. Ozilgen, *Handbook of Food Process Modeling and Statistical Quality Control*, 2nd ed. Boca Raton, FL, USA: CRC Press, 2011.

[5] M. Riaz, "Control charting and survey sampling techniques in process monitoring," *J. Chin. Inst. Eng.*, vol. 38, no. 3, pp. 342–354, Apr. 2015.

[6] S. A. Abbasi, M. Riaz, A. Miller, S. Ahmad, and H. Z. Nazir, "EWMA dispersion control charts for normal and non-normal processes," *Qual. Rel. Eng. Int.*, vol. 31, no. 8, pp. 1691–1704, Dec. 2015.

[7] D. Driankov, H. Hellendoorn, and M. Reinfrank, *An Introduction to Fuzzy Control*. New York, NY, USA: Springer, 1993.

[8] A. Faraz and M. B. Moghadam, "Fuzzy control chart a better alternative for Shewhart average chart," *Qual. Quantity*, vol. 41, no. 3, pp. 375–385, Apr. 2007.

[9] M. Gülbay, C. Kahraman, and D. Ruan, "α-cut fuzzy control charts for linguistic data," *Int. J. Intell. Syst.*, vol. 19, no. 12, pp. 1173–1195, Dec. 2004.

[10] S. Fadaei and A. Pooya, "Fuzzy U control chart based on fuzzy rules and evaluating its performance using fuzzy OC curve," *TQM J.*, vol. 30, no. 3, pp. 232–247, May 2018.

[11] N. P. Alakoc and A. Apaydin, "A fuzzy control chart approach for attributes and variables," *Eng., Technol. Appl. Sci. Res.*, vol. 8, no. 5, pp. 3360–3365, Oct. 2018.

[12] F. Smarandache, ‘‘Neutrosophic set–a generalization of the intuitionistic fuzzy set,’’ in *Proc. IEEE Int. Conf. Granular Comput.*, 2006, vol. 24, no. 3, pp. 38–42.
[13] J. Ye, ‘‘Similarity measures between interval neutrosophic sets and their applications in multicriteria decision-making,’’ *J. Intell. Fuzzy Syst.*, vol. 26, no. 1, pp. 165–172, 2014.
[14] M. Aslam and O. Arif, ‘‘Testing of grouped product for the Weibull distribution using neutrosophic statistics,’’ *Symmetry*, vol. 10, no. 9, p. 403, Sep. 2018.
[15] J. Morán, J. Chuga, and W. M. Arias, ‘‘Neutrosophic statistics applied to the analysis of socially responsible participation in the community,’’ *Neutro. Sets Syst.*, vol. 26, no. 1, pp. 26–28, 2019.
[16] J. Chen, J. Ye, S. Du, and R. Yong, ‘‘Expressions of rock joint roughness coefficient using neutrosophic interval statistical numbers,’’ *Symmetry*, vol. 9, no. 7, p. 123, Jul. 2017.
[17] M. Aslam, ‘‘A new sampling plan using neutrosophic process loss consideration,’’ *Symmetry*, vol. 10, no. 5, p. 132, Apr. 2018.
[18] M. Aslam and M. A. Raza, ‘‘Design of new sampling plans for multiple manufacturing lines under uncertainty,’’ *Int. J. Fuzzy Syst.*, vol. 21, no. 3, pp. 978–992, Apr. 2019.
[19] M. Aslam, R. A. R. Bantan, and N. Khan, ‘‘Design of NEWMA np control chart for monitoring neutrosophic nonconforming items,’’ *Soft Comput.*, vol. 24, no. 21, pp. 16617–16626, Nov. 2020.
[20] Z. Khan, M. Gulistan, W. Chammam, S. Kadry, and Y. Nam, ‘‘A new dispersion control chart for handling the neutrosophic data,’’ *IEEE Access*, vol. 8, pp. 96006–96015, 2020.
[21] Z. Khan, M. Gulistan, R. Hashim, N. Yaqoob, and W. Chammam, ‘‘Design of S-control chart for neutrosophic data: An application to manufacturing industry,’’ *J. Intell. Fuzzy Syst.*, vol. 38, no. 4, pp. 4743–4751, Apr. 2020.
[22] M. Aslam, R. A. R. Bantan, and N. Khan, ‘‘Design of a new attribute control chart under neutrosophic statistics,’’ *Int. J. Fuzzy Syst.*, vol. 21, no. 2, pp. 433–440, Mar. 2019.
[23] Z. Khan, M. Gulistan, S. Kadry, Y. Chu, and K. Lane-Krebs, ‘‘On scale parameter monitoring of the Rayleigh distributed data using a new design,’’ *IEEE Access*, vol. 8, pp. 188390–188400, Oct. 2020.
[24] D. Hoffman and O. J. Karst, ‘‘The theory of the Rayleigh distribution and some of its applications,’’ *J. Ship Res.*, vol. 19, no. 3, pp. 172–191, Sep. 1975.
[25] M. P. Hossain, M. H. Omar, M. Riaz, and S. Y. Arafat, ‘‘On designing a new control chart for Rayleigh distributed processes with an application to monitor glass fiber strength,’’ *Commun. Statist.-Simul. Comput.*, pp. 1–17, Jan. 2020, doi: 10.1080/03610918.2019.1710192.
[26] S. Dey, T. Dey, and D. Kundu, ‘‘Two-parameter Rayleigh distribution: Different methods of estimation,’’ *Amer. J. Math. Manage. Sci.*, vol. 33, no. 1, pp. 55–74, Jan. 2014.
[27] F. Figueiredo and M. I. Gomes, ‘‘The skew-normal distribution in SPC,’’ *REVSTAT-Stat. J.*, vol. 11, no. 1, pp. 83–104, Mar. 2013.
[28] Z. Abbas, H. Z. Nazir, N. Akhtar, M. Riaz, and M. Abid, ‘‘On developing an exponentially weighted moving average chart under progressive setup: An efficient approach to manufacturing processes,’’ *Qual. Rel. Eng. Int.*, vol. 36, no. 7, pp. 2569–2591, Nov. 2020.
[29] S. A. Abbasi and N. A. Adegoke, ‘‘Auxiliary-information-based efficient variability control charts for phase I of SPC,’’ *Qual. Rel. Eng. Int.*, vol. 36, no. 7, pp. 2322–2337, Nov. 2020.
[30] S. M. Anwar, M. Aslam, M. Riaz, and B. Zaman, ‘‘On mixed memory control charts based on auxiliary information for efficient process monitoring,’’ *Qual. Rel. Eng. Int.*, vol. 36, no. 6, pp. 1949–1968, Oct. 2020.
[31] J. Lieblein and M. Zelen, ‘‘Statistical investigation of the fatigue life of deep-groove ball bearings,’’ *J. Res. Bur. Standards*, vol. 57, no. 5, pp. 273–316, 1956.
[32] C. Caroni, ‘‘The correct ‘ball bearings’ data,’’ *Lifetime Data Anal.*, vol. 8, no. 4, pp. 395–399, 2002.
[33] S. Dey and T. Dey, ‘‘Statistical inference for the Rayleigh distribution under progressively type-II censoring with binomial removal,’’ *Appl. Math. Model.*, vol. 38, no. 3, pp. 974–982, Feb. 2014.
[34] M. Z. Raqab, ‘‘Inferences for generalized exponential distribution based on record statistics,’’ *J. Stat. Planning Inference*, vol. 104, no. 2, pp. 339–350, Jun. 2002.

ZAHID KHAN received the Ph.D. degree from University Technology PETRONAS, Malaysia, in 2017. He is currently an Assistant Professor with the Department of Mathematics and Statistics, Hazara University Mansehra, Pakistan. His research interests include fuzzy statistics and statistical methods for industrial process control.

MUHAMMAD GULISTAN received the M.Phil. degree from Quaid-i-Azam University Islamabad, in 2011, and the Ph.D. degree from Hazara University Mansehra, in 2016. He is currently working as an Assistant Professor with the Department of Mathematics and Statistics, Hazara University Mansehra. He supervised over 25 M.Phil. and five Ph.D. research students. He has published more than 60 research articles in different well reputed journals. His research interests include cubic sets and their generalizations, non-associative hyper structures, neutrosophic cubic sets, neutrosophic cubic graphs, and decision making.

NASREEN KAUSAR received the Ph.D. degree in mathematics from Quaid-i-Azam University Islamabad, Pakistan. She is currently an Assistant Professor of mathematics with the University of Agriculture, Faisalabad, Pakistan. Her research interests include the numerical analysis and numerical solutions of the ordinary differential equations (ODEs), partial differential equations (PDEs), volterra integral equations, and associative and commutative/non-associative and non-commutative fuzzy algebraic structure and their applications.

CHOONKIL PARK received the Ph.D. degree in mathematics from the University of Maryland, in 1996. He is currently a Distinguished Professor with the Department of Mathematics, Research Institute of Natural Sciences, Hanyang University, Seoul, South Korea. His research and publication interests include functional analysis, fixed point theory, and rough and soft set theory.